DTIC COPY

REPORT DOCUMENTATION PAGE	Form Approved OMB No. 0704-01-0188

1. REPORT DATE (DD-MM-YYYY)	14-05-2009
2. REPORT TYPE	REPRINT
3. DATES COVERED (From - To)	
4. TITLE AND SUBTITLE	Dependence of Electron Flux on Electron Temperature in Spacecraft Chargilng
5a. CONTRACT NUMBER	
5b. GRANT NUMBER	
5c. PROGRAM ELEMENT NUMBER	62601F
5d. PROJECT NUMBER	1010
5e. TASK NUMBER	RS
5f. WORK UNIT NUMBER	A1
6. AUTHORS	Shu T. Lai
7. PERFORMING ORGANIZATION NAME(S) AND ADDRESS(ES)	Air Force Research Laboratory /RVBXT 29 Randolph Road Hanscom AFB, MA 01731-3010
8. PERFORMING ORGANIZATION REPORT NUMBER	AFRL-RV-HA-TR-2009-1041
9. SPONSORING/MONITORING AGENCY NAME(S) AND ADDRESS(ES)	
10. SPONSOR/MONITOR'S ACRONYM(S)	AFRL/RVBXT
11. SPONSOR/MONITOR'S REPORT NUMBER(S)	
12. DISTRIBUTION/AVAILABILITY STATEMENT	Approved for Public Release; distribution unlimited.
13. SUPPLEMENTARY NOTES	Reprinted from *Journal of Applied Physics, Vol. 105, 094912 (2009) doi:10.1063/1.3125517* 66ABW-2008-0451

14. ABSTRACT

Two important observations when the onset of spacecraft surface charging occurs are (1) the electron flux measured in the high-energy (above several keV) channels onboard rises and (2) the ambient electron temperature rises above a critical value. We show by means of an analytical model that the two behaviors are consistent with each other.

15. SUBJECT TERMS

20110509003

16. SECURITY CLASSIFICATION OF: a. REPORT	b. ABSTRACT	c. THIS PAGE	17. LIMITATION OF ABSTRACT	18. NUMBER OF PAGES	19a. NAME OF RESPONSIBLE PERSON	19B. TELEPHONE NUMBER (Include area code)
UNCL	UNCL	UNCL	UNL	9	Shu T. Lai	

Dependence of electron flux on electron temperature in spacecraft charging

Shu T. Lai[a)]
AFRL/RVBXT, Hanscom, AFB., Massachusetts 01731, USA

(Received 20 January 2009; accepted 2 April 2009; published online 14 May 2009)

Two important observations when the onset of spacecraft surface charging occurs are (1) the electron flux measured in the high-energy (above several keV) channels onboard rises and (2) the ambient electron temperature rises above a critical value. We show by means of an analytical model that the two behaviors are consistent with each other. [DOI: 10.1063/1.3125517]

I. INTRODUCTION

It has been observed repeatedly on the Spacecraft Charging at High Altitudes (SCATHA) satellite that when spacecraft surface charging occurred, the electron fluxes measured in the channels of above several keV rose while those measured in the low energy channels below several keV fell. In cases of severe charging, the rise in flux obtained in the channels of about 20–30 keV was remarkable and had received much attention.[1] These observations have led to some widespread belief that a rise in the flux of the 20–30 keV channel is one of the best symptoms to signal the occurrence of spacecraft charging. On the other hand, one can show analytically by means of the Maxwellian model[2–6] that spacecraft charging occurs when the ambient electron temperature rises above a critical temperature and that the charging level increases as the temperature rises further. Observations on the Los Alamos National Laboratory (LANL) geosynchronous satellites have provided abundant evidences supporting the temperature dependence idea of spacecraft charging.[7,8] Each of the two behaviors mentioned above is important, but, like the Indian fable of four blind persons touching an elephant, the two behaviors seem to be unrelated aspects in spacecraft charging. Some even thought that the two ideas are mutually exclusive. The purpose of this note is to show in a theoretical framework that the two behaviors are mutually consistent. In the next section, we begin with the definition of flux, develop the analytical formulation, and present numerical solutions and their physical interpretations.

II. MAXWELLIAN FLUX

The flux J is defined in terms of the Maxwellian velocity distribution $F(v)$ of the electrons,

$$J = \int d^3v \mathbf{v} F(v). \tag{1}$$

In Eq. (1), the velocity distribution $F(v)$ is given by

$$F(v) = n\left(\frac{m}{2\pi kT}\right)^{3/2} \exp\left(-\frac{mv^2}{2kT}\right). \tag{2}$$

The velocity v can be expressed[9] in terms of energy E with the substitution $E=(1/2)mv^2$. After the substitution, Eq. (2) is converted to the Maxwellian–Boltzmann distribution $f(E)$ of the ambient electrons,

$$f(E) = n\left(\frac{m}{2\pi kT}\right)^{3/2} \exp\left(-\frac{E}{kT}\right), \tag{3}$$

where T is the electron temperature, m the electron mass, and E the electron energy. Figure 1 shows a plot of $\log_e f(E)$ versus E. The plot shows a straight line and its slope equals $-1/kT$. The y intercept at $E=0$ is given by

$$f(0) = n\left(\frac{m}{2\pi kT}\right)^{3/2}, \tag{4}$$

which is a function of the density n and the Maxwellian temperature T of the ambient electrons. As the temperature T changes, the location of the y intercept changes. Note that one can use $\log_{10} f(E)$ and the plot would be a straight line,

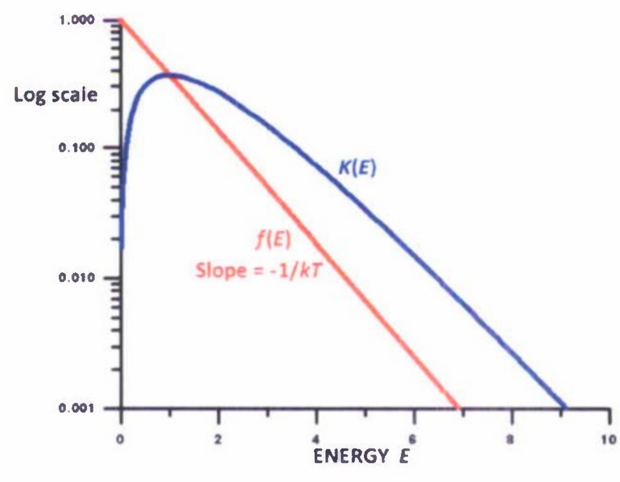

FIG. 1. (Color online) Log of the Maxwellian energy distribution function plotted against energy E. The slope of the straight line depends on the temperature T. The y intercept is a function of the density n and the temperature T. A plot of log $K(E)$ vs E is also plotted. It features a maximum at $E=T$. (For simplicity, both n and T equal 1 in the input. To show the correct slope, one needs to use the natural log scale.)

[a)]Electronic mail: afrl.rvb.pa@hanscom.af.mil.

but there is a multiplicative constant because $\log_e f(E) = \log_e 10 \times \log_{10} f(E)$.

For normal incidence, the flux J of Eq. (1) can be simplified. Neglecting the multiplicative constant of π and m, which do not vary during spacecraft charging, we write the normal flux J [Eq. (3)] as a function of $f(E)$,

$$J = \int_0^{\infty} dE E f(E). \tag{5}$$

The flux J, Eq. (5), can be written as

$$J = \int_0^{\infty} dE \frac{dJ(E)}{dE}, \tag{6}$$

where the kernel (dJ/dE) of the integral, Eq. (5), is called the differential flux $K(E)$,

$$K(E) = \frac{dJ(E)}{dE} = Ef(E). \tag{7}$$

A plot of log $K(E)$ is shown in Fig. 1.

III. MEASUREMENT TECHNIQUE

In practice, the instruments for flux measurement on satellites have limitations. Instead of obtaining a continuous distribution of flux $J(E)$ as a function of energy, the measurement obtains the flux in discrete energy channels, each channel having its finite energy range ΔE. That is, the measurement gives $\Delta J(E)/\Delta E$, where Δ represents a finite increment. We can rewrite Eq. (5) as follows:

$$J = \sum_i \left(\frac{\Delta J(E)}{\Delta E}\right)_i \Delta E_i = \sum_i K_i(E) \Delta E_i, \tag{8}$$

where $[\Delta J(E)/\Delta E]_i$, denoted by $K_i(E)$, is the differential flux in the ith channel,

$$K_i(E) = \left(\frac{\Delta J(E)}{\Delta E}\right)_i. \tag{9}$$

An example of differential flux measurements is shown in Fig. 2. In this example, the ambient flux is measured in discrete energy channels. The ith channel measures the differential flux $K_i(E)$ at $E_i \pm \Delta E_i$.

IV. DILEMMA

Each of the two techniques for signaling the occurrence of spacecraft charging has received credible observational evidence. In the high energy channel technique, when a high energy channel, such as 20–30 keV, rises relative to the lower energy channels (keV or less), spacecraft charging occurs (Fig. 2). In the critical temperature technique, when the ambient electron temperature rises above a critical value, charging occurs (Fig. 3). We will not attempt to simulate case-specific results because more parameters are often needed. We point out that both techniques have received concrete evidence obtained in space and yet they seem to be unrelated to each other. There is need to bridge an understanding concerning both techniques.

While there is a Maxwellian model[2–8] for explaining the physics in the "critical temperature" technique, the high energy channel technique is based solely on experimentalist's observations. We will attempt to prove the mutual consistency of the two techniques in the following sections.

Before we discuss flux, let us examine the relation of a Maxwellian distribution $f(E)$, Eq. (1), with temperature. Since the slope, $d[\log_e f(E)]/dE$, equals $-1/kT$, rising temperature would correspond to higher population at high energies and lower population at low energies [Fig. 4(a)]. For two temperatures T_1 and $T_2(>T_1)$, the transition energy E_t, at which the distribution $f(E_t)$ is unchanged, is given by

$$E_t = \frac{(3/2)\log_e(T_2/T_1)}{(1/kT_1) - (1/kT_2)}. \tag{10}$$

If the distribution deviates from Maxwellian and one can still fit an average slope to the curve of $f(E)$, the "critical temperature" technique is still approximately valid. If the distribution deviates in an unmanageable manner, temperature is undefined [Fig. 4(b)] and a manageable way to characterize the electron distribution may be impossible.

V. EFFECT OF RISING TEMPERATURE ON THE NET INCOMING FLUX

First, to examine the effect of rising temperature T on the net incoming flux $K(E)$ in a channel, we differentiate Eq. (7) by T,

$$\frac{\partial K(E,T)}{\partial T} = \left(E - \frac{3}{2}kT\right)\frac{1}{(kT)^2}K(E). \tag{11}$$

This simple result, Eq. (11), reveals an interesting behavior. The temperature gradient of differential flux, $K(E)$, is negative for E below $(3/2)kT$ but positive for E above $(3/2)kT$. As the temperature rises, the differential flux K increases for T below $2E/3$ but decreases for T above $2E/3$. At $kT = 2E/3$, the differential flux is maximum. Figure 5 illustrates the effect.

Next, to seek out the most sensitive channel for a given temperature, we differentiate $K(E)$ by E,

$$\frac{\partial K(E,T)}{\partial E} = \left(1 - \frac{E}{kT}\right)f(E). \tag{12}$$

Equation (12) reveals that the differential flux increases with the energy E as long as E is below kT. For E above kT, the differential flux decreases as the energy increases. The maximum of the differential flux K is at $E=kT$. Figure 7 illustrates the effect.

With spacecraft charging to a potential ϕ (negative volt), the incoming electron flux is reduced by the Boltzmann factor, $\exp(-q_e\phi/kT)$,

$$K(E,T) = Ef(E)\exp\left(-\frac{q_e\phi}{kT}\right). \tag{13}$$

Accordingly, the location of the zero gradient of Eq. (11) is shifted by $q_e\phi$, where q_e is the charge of electron. That is, the location of Max$[\partial K/\partial T]$ is given by

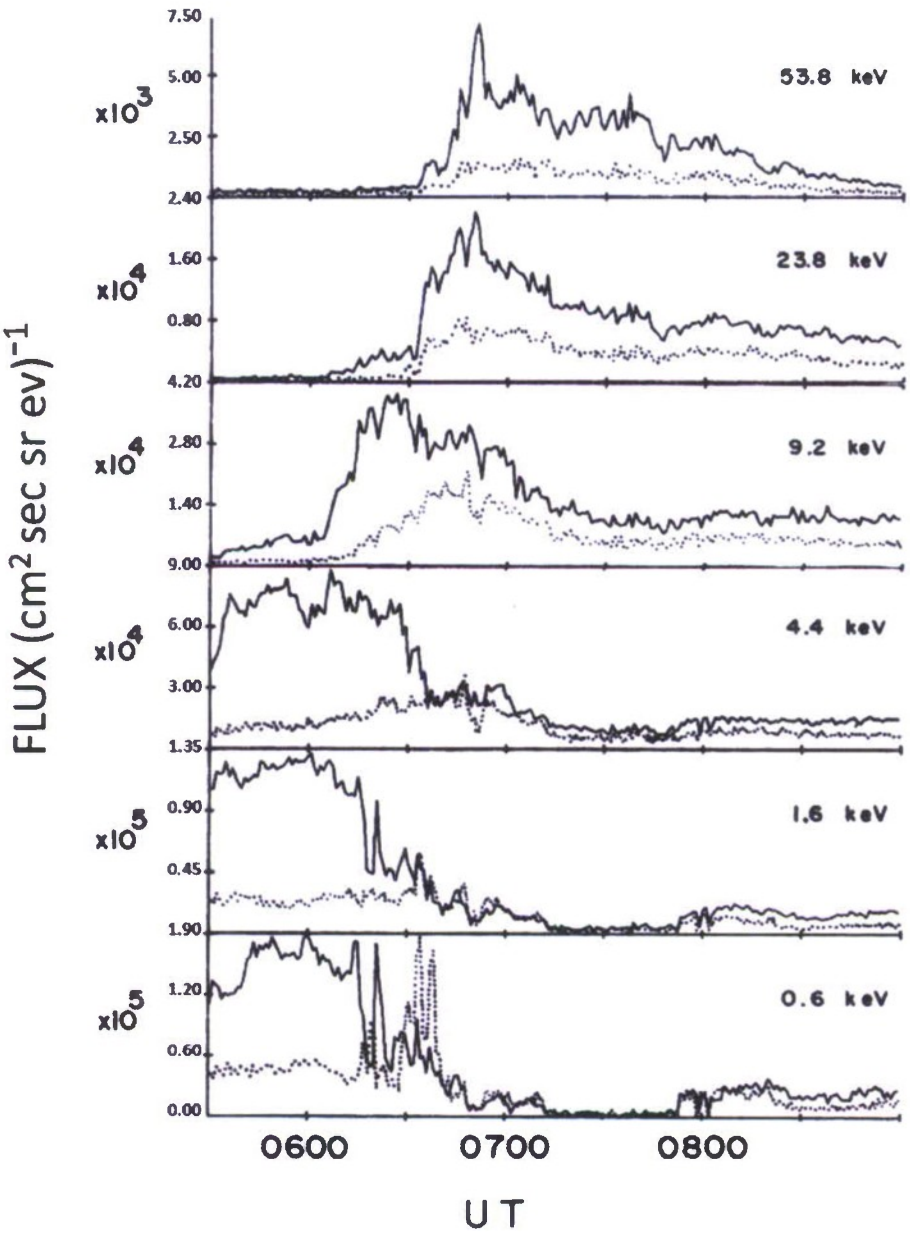

FIG. 2. Fluxes measured in channels of different energies before and after a significant charging event. Charging occurs at 6:30 to about 7:00UT. The temperature of the main component Maxwellian rises from 9.2 keV (6:30UT) to 23 keV (6:50UT) (from Ref. 1).

$$E + q_e\phi - \frac{3}{2}kT = 0. \tag{14}$$

The location of Max$[\partial K/\partial E]$ given by Eq. (12) is unchanged by the potential ϕ.

VI. RESULTS

We have obtained numerical results in the theoretical framework of Maxwellian plasmas. Figure 5 shows the calculated differential flux $K(E,T)$ as a function of temperature T for various energies corresponding to typical channel energy values. The spacecraft potential is assumed to be zero. The lowest energy channel (0.6 keV) shows the highest flux and the higher energy channel shows lower fluxes, as one expects from the general nature of Maxwellian or any equilibrium distributions. At higher temperatures, the fluxes at higher energy (E=9.2, 23.8 keV) channels rise whereas those at lower energies fall. For a given energy E, the maximum of the flux curve is located at $T=(2E/3)$, in agreement with Eq. (11).

Figure 6 shows the same curves but with the spacecraft potential equal to −4 kV. Physically, the fluxes of the low energy channels (E=0.6, 1.6 keV) are suppressed clearly because the low energy ambient electrons can hardly reach the spacecraft that is charged. Mathematically, the flux reduction is by the multiplicative Boltzmann factor. The maxima of the curves are no longer at $T=(2E/3)$ but at $T=2(E+q_e\phi)/3$, in agreement with Eq. (14). A prominent feature in this figure is the relative enhancement of the fluxes in the higher energy channels.

Figure 7 shows the fluxes as a function of energy for various given temperatures. The spacecraft is considered to be uncharged. As expected from Fig. 2, the higher energy

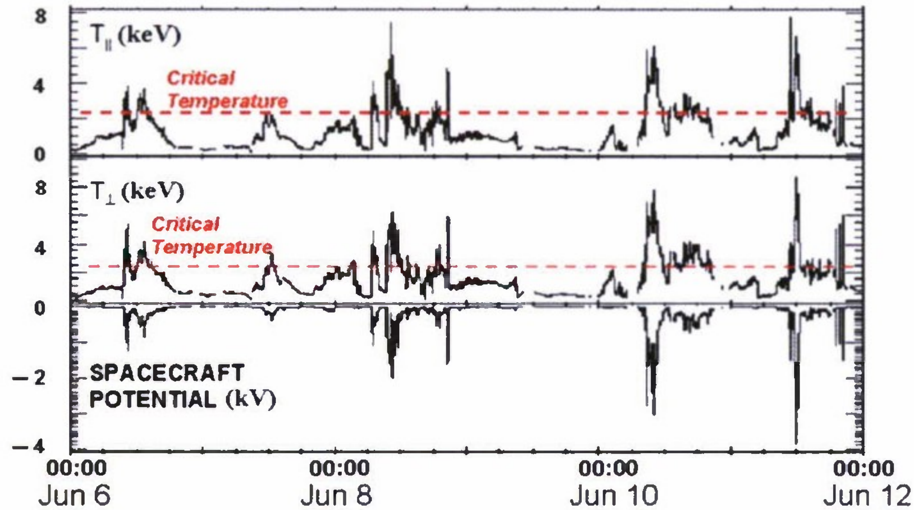

FIG. 3. (Color online) Charging on the famous Bastille Day event, 2000. The spacecraft potential (negative kV) rises whenever the electron temperature exceeds a critical value (from Ref. 7).

electron population increases with the temperature and so do the high energy fluxes, whereas the low energy fluxes do oppositely. The maximum of each curve is located at $E=T$, in agreement with Eq. (12). Note also that the area under the curve $K(E)$ is given by the following integral:

$$\int_0^\infty dEK(E) = \int_0^\infty dEEn\left(\frac{m}{2\pi kT}\right)^{3/2}\exp\left(-\frac{E}{kT}\right)$$
$$= n\left(\frac{m}{2\pi kT}\right)^{3/2}T^2\left[\exp\left(-\frac{E}{kT}\right)\left(-\frac{E}{kT}-1\right)\right]_0^\infty. \tag{15}$$

The square bracket in Eq. (15) is unity. Therefore, the integral of Eq. (15) is proportional to $T^{1/2}$. That is, the flux J increases as the electron temperature T increases, as expected.

Figure 8 shows the same curves as in Fig. 7 but with the spacecraft potential at −4 kV. Again, the suppression of the low energy fluxes is because of the Boltzmann factor. The higher energy (E=9.2,23.8 keV) fluxes at 20-30 keV, for example, are enhanced relatively.

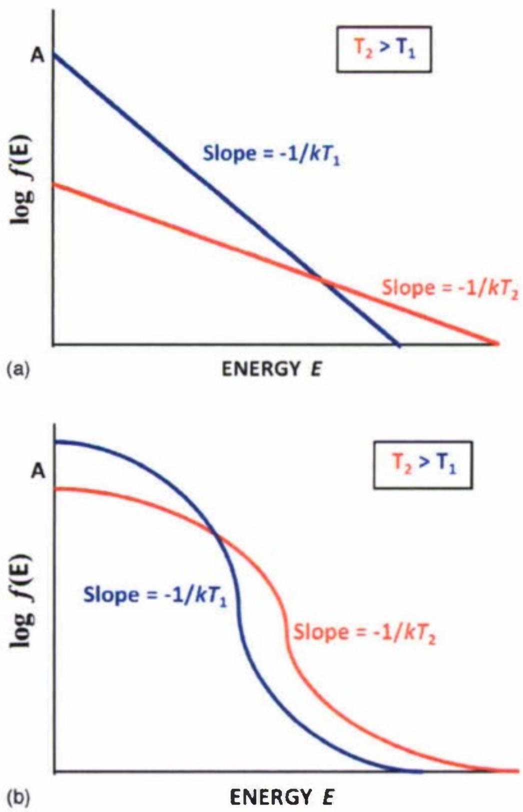

FIG. 4. (Color online) (a) Log of the Maxwellian energy distribution function plotted against energy E for two different temperatures. As temperature increases, both the intercept and the slope decrease. The function increases for E exceeding $3kT/2$. (b) Deviation from Maxwellian. If the deviation is gentle, an average slope can still be defined. The idea of "higher temperature increases the high energy population" is still valid. For distributions with unmanageable deviations, temperature is undefined.

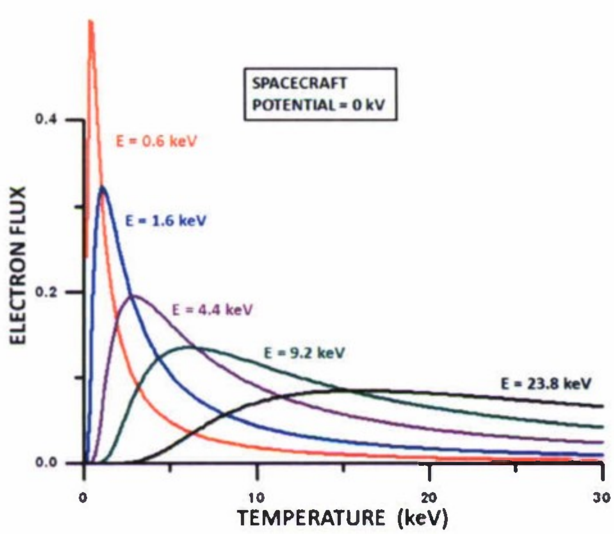

FIG. 5. (Color online) Flux in four energy channels as a function of electron temperature T. The spacecraft is uncharged. As the energy E rises, the flux maximum at $T=2E/3$ shifts to the right hand side.

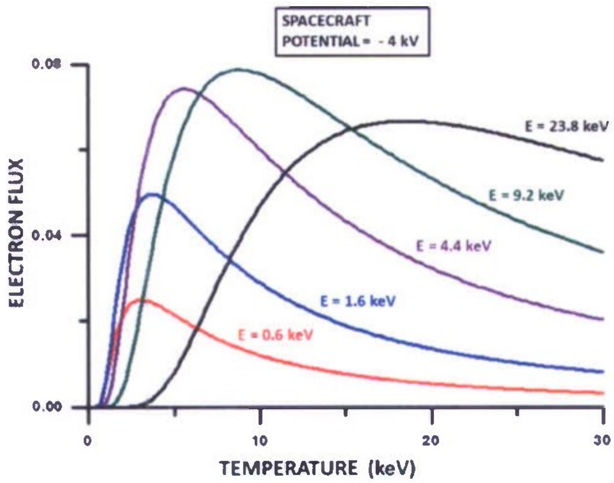

FIG. 6. (Color online) Flux in four energy channels as a function of electron temperature T. The spacecraft is charged to −4 kV. As the energy E rises, the flux maximum shifts to higher value of T.

VII. CONCLUSION

From this study, we conclude that the ideas of rising temperature and relative enhancement of high energy fluxes are not mutually exclusive. Even without spacecraft charging, the high energy channel fluxes increase with the ambient electron temperature. Furthermore, if spacecraft charging occurs, the low energy channel fluxes are suppressed relative to the high energy channels because of Coulomb repulsion rendering the enhancement of the high energy channel fluxes

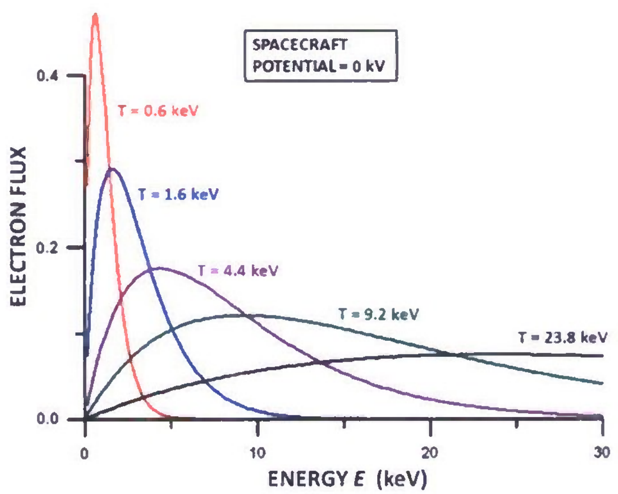

FIG. 7. (Color online) Differential flux as a function of energy at various temperatures. The spacecraft is uncharged (ϕ=0). Note that the maximum of each curve is at $E=kT$.

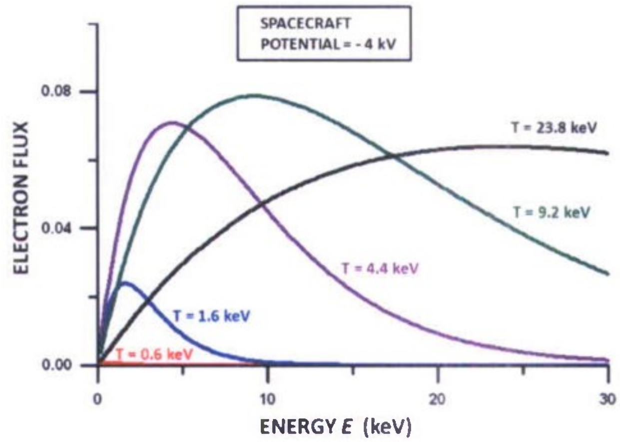

FIG. 8. (Color online) Same caption as the previous figure, but the spacecraft potential is −4 kV. The amplitude Is reduced by $\exp(-q_e\phi/kT)$. Note that the maximum of each curve is at $E=kT$ and the flux of T=0.6 keV Is reduced to practically zero.

more prominent. Whereas the method of critical temperature[2–6] gives precise signaling of the onset of spacecraft charging as verified[7,8] by the Los Alamos National Laboratory (LANL) geosynchronous satellite data, the method of flux enhancement at high energies[1] gives prominent signals when charging occurs but without the precision of the onset of charging. It would be misleading to interpret from the rising flux in the 20–30 keV channels during spacecraft charging that only the 20–30 keV electrons are responsible for charging. It is advisable to "see the full picture" by considering the entire electron energy distribution for modeling and forecasting spacecraft charging.

ACKNOWLEDGMENTS

The author is grateful to Henry Garrett and David Cooke for discussions.

[1] M. S. Gussenhoven and E. G. Mullen, J. Spacecr. Rockets **20**, 26 (1982).
[2] S. T. Lai, M. S. Gussenhoven, and H. A. Cohen, EOS Trans. Am. Geophys. Union **63**, 421 (1982).
[3] J. G. Laframboise, R. Godard, and M. Kamitsuma, Multiple Floating Potentials, *Proceedings of International Symposium on Spacecraft Materials in Space Environment*, Toulouse, France, 1982, pp. 269–275.
[4] S. T. Lai, M. S. Gussenhoven, and H. A. Cohen, in *Proceedings of the 17th ESLAB Symposium*, edited by D. Guyenne and J. H. A. Pedersen (European Space Agency, Noordwijk, The Netherlands, 1983), pp. 169–175.
[5] J. G. Laframboise and M. Kamitsuma, *Proceedings of Air Force Geophysics Workshop on Natural Charging of Large Space structures in Near Earth Polar Orbit*, 1983, AFRL-TR-83-0046, ADA-134894, pp. 293–308.
[6] S. T. Lai, IEEE Trans. Nucl. Sci. **19**, 1629 (1991).
[7] S. T. Lai and D. Della-Rose, J. Spacecr. Rockets **38**, 922 (2001).
[8] S. T. Lai and M. Tautz, J. Geophys. Res. **111**, A09201 (2006).
[9] J. L. Shohet, *The Plasma State* (Academic, New York, 1971).